The Open Bioinformatics Journal
DOI: 10.2174/0118750362391710250929194610, 2025, 18, e18750362391710

ISSN: 1875-0362
1

RESEARCH ARTICLE **OPEN ACCESS**

MPFAN: A Novel Multiscale Network for Brain Tumor MRI Classification

Shahnawaz Ahmad[1], Mohd. Aquib Ansari[1,£], Arvind Mewada[1], Prabhishek Singh[1], Manoj Diwakar[2,3], Salman Akhtar[4,*] and Basu Dev Shivahare[5]

[1]*School of Computer Science, Engineering & Technology, Bennett University, Greater Noida, India*
[£]*Present Address: School of Computer Science and Engineering, Galgotias University, Greater Noida, India*
[2]*CSE Department, Graphic Era deemed to be University, Dehradun, Uttarakhand, India*
[3]*Graphic Era Hill University, Dehradun, Uttarakhand, India*
[4]*Department of Bioengineering Integral University, Lucknow, India*
[5]*School of Computer Science and Engineering, Galgotias University, Greater Noida, India*

Abstract:

Introduction: Accurate classification of brain tumours using MRI scans is vital for early diagnosis and treatment. However, conventional deep learning models often require complete MRI sequences, which can prolong scan times and lead to patient discomfort or motion-related image degradation. Thus, enhancing diagnostic accuracy under faster scanning conditions is a critical research need. Therefore, this research aims to show how our proposed mechanism, namely Multiscale Parallel Feature Aggregation Network (MPFAN), accurately improves the diagnosis of classifying brain tumours while maintaining Magnetic Resonance Imaging (MRI) quality in fast MRI scanning.

Methods: This article proposed an MPFAN architecture that utilizes parallel branches to extract image features from different scales, using independent pathways with varied filters and movement steps. Feature combination blocks, feedback prevention mechanisms, and strict training constraints enhance system reliability.

Results: MPFAN achieved an accuracy of 97.4%, outperforming many existing brain tumour classification models. Performance improved steadily over training epochs, and optimizer comparisons showed Adam and Ada-Delta yielded the best results. Ablation studies confirmed that multiscale feature extraction, dropout regularization, and feature fusion significantly contribute to classification accuracy.

Discussion: The MPFAN model demonstrates superior performance due to its ability to effectively extract and integrate multiscale features. Its dual-branch architecture enables deeper contextual understanding, and its high accuracy validates its clinical potential. However, the model's reliance on a single dataset and potential overfitting in later training epochs indicate the need for broader validation and optimization in real-world clinical environments.

Conclusion: The proposed MPFAN architecture enhances brain tumour classification by improving image processing efficiency and decision-making speed, making it a reliable and effective diagnostic tool.

Keywords: Brain tumour classification, Multiscale feature aggregation, Deep neural network, Medical image processing, Computer-aided diagnosis, MRI, MPFAN.

* Address correspondence to this author at the Department of Bioengineering Integral University, Lucknow, India;
E-mail: salmanakhtar18@gmail.com

Cite as: Ahmad S, Ansari M, Mewada A, Singh P, Diwakar M, Akhtar S, Shivahare B. MPFAN: A Novel Multiscale Network for Brain Tumor MRI Classification. Open Bioinform J, 2025; 18: e18750362391710.
http://dx.doi.org/10.2174/0118750362391710250929194610

Received: March 10, 2025
Revised: June 26, 2025
Accepted: July 09, 2025
Published: October 07, 2025

1. INTRODUCTION

Brain tumours are extremely dangerous and fatal cancers, which cause loss of life. Ageing or damaged brain cells that fail to regenerate properly may create extra tissue, leading to tumour formation [1]. Brain tumours exist in two forms: cancerous growths that spread and non-cancerous growths that do not. Fast detection and treatment of malignant brain tumours have become essential since they spread rapidly into nearby brain tissues to increase the chances of survival [2].

Doctors often choose MRI scans to discover brain tumours because these devices create precise brain images through magnets instead of radiation exposure. Brain tumours are generally categorized into three types based on their location: meningiomas, pituitary tumours, and gliomas [3]. There are two main brain tumour image classification strategies using MRI scans: traditional manual feature analysis and deep learning techniques. Doctors must select image features by hand before feeding them into standard classifiers, including Support Vector Machine (SVM) and K-Nearest Neighbour (KNN). These methods work well but take a long time to process data and require a lot of effort [4-7]. Convolutional Neural Networks (CNNs) enable deep learning systems to automatically identify and organize features while addressing challenges related to improper data and slow processing.

Standard deep learning approaches need all the information within the MRI images to perform classification. Extended MRI procedures make patients uncomfortable and result in damaged MRI images when patients move. Deep learning methods for fast MRI scanning must improve their ability to preserve image quality to achieve better brain tumour classification results [8, 9].

Our proposed MPFAN architecture combines CNN features from different scales through parallel networks to boost brain tumour classification results. MPFAN uses parallel branches to extract detailed image features both near and far. The system uses two independent pathways to examine input images using different filters and movement steps to produce different feature sets. Integrating separate feature combination blocks, feedback prevention tools, and strict training limits helps the system perform more reliably. The proposed method combines efficient brain tumour classification with powerful diagnostic results through better processing and quicker decision-making. The main contribution of the paper is as follows:

- We present a state-of-the-art method to classify brain tumours from MRI images.
- We present a Multiscale Parallel Feature Aggregation Network (MPFAN) to detect tumours efficiently from medical images.
- We experimentally explore this network for different parameters.

1.1. Related Work

The current literature on glioma grading and brain tumour classification predominantly relies on CNN-based methods due to their ability to learn local features. However, these methods struggle with modelling long-range dependencies and global context, which may limit classification accuracy. The machine learning-based approach discussed by Wang *et al.* demonstrates satisfactory accuracy but provides limited insights into general performance across various tumour classes [10].

Attention mechanisms have increased the emphasis on features, yet convolutional operations still dominate, making capturing objects such as blurred edges or intensity variations challenging. On the other hand, previous approaches achieve high accuracy; further enhancements are needed to develop more general and multiscale classifiers. Rasheed *et al.* employed an efficient CNN method to categorize three different types of brain tumors [11]. Abd El-Wahab *et al.* proposed a deep learning model called BTC-FCNN to enhance classification accuracy while reducing the computational overhead of MRI-based classifiers [12].

Ozkaraca *et al.* utilized Dense CNN to improve brain tumour classification in MRI imaging [13]. Similarly, Muezzinoglu and Others introduced PatchResNet, a framework leveraging multi-sized patch-based feature fusion to achieve high classification accuracy [14]. Their approach incorporates KNN classification and iterative hard voting, which are crucial for boosting accuracy. Mijwil *et al.* employed MobileNetV1 to classify brain tumors in MRI images, demonstrating an accurate and efficient model for medical imaging systems [15]. Saurav *et al.* introduced a simple attention-guided convolutional neural network (AG-CNN) architecture that utilizes channel attention and global average pooling (GAP) as its feature extraction mechanism [16].

Sekhar *et al.* adopted the GoogLeNet model and employed SVM and KNN classifiers to differentiate gliomas, meningiomas, and pituitary tumors [4]. Athisayamani *et al.* utilized ResNet152 to enhance feature extraction and reduce dimensionality, improving classification performance [17]. Shahin *et al.* designed MBTFCN, which classifies tumors across multiple categories using three key techniques, including feature extraction with residual connections and attention mechanisms [18].

In their research, Aloraini *et al.* integrated Transformer and CNN elements into a single model, while Zulfiqar *et al.* leveraged EfficientNets for brain tumor image classification [19, 20]. Mehnatkesh *et al.* [21] applied an improved ant colony algorithm to optimize MRI tumor classification using ResNet. Singh and Agarwal developed a CNN-based approach specifically designed for T1WCE MRI images [22].

Isunuri and Kakarla utilized a neural network based on separable convolution to maximize computational speed in tumor classification [23]. Raza *et al.* extended GoogLeNet into a 15-layer deep network to enhance expressive

capabilities [24]. Aamir *et al.* employed EfficientNet-B0 for feature extraction after grouping and segmenting images, enhancing image contrast using nonlinear techniques [25].

A new approach, referred to as full-stack learning (FSL), was proposed by Wang *et al.*, where sampling, reconstruction, and segmentation are co-performed due to task dependencies and improve MRI workflow [26]. Ling *et al.* proposed a new multitask attention network named MTANet for better segmentation and classification, together with an attention mechanism [27]. Wang *et al.* developed a multi-stage hybrid attention network (MHAN) model to conduct MRI image super-resolution and reconstruction, besides having specialized modules regarding enhanced spatial feature extraction [28]. Sui *et al.* applied ConvNext blocks in a multi-task learning system for liver MRI analysis and found refined details for higher accuracy [29]. Subsequently, Delannoy *et al.* proposed SegSRGAN, which employs the GANs to improve the resolution in neonatal brain MRI and the segmentation accuracy [30]. Corona *et al.* integrated total variation reconstruction and Chan-Vesed segmentation using nonconvex Bregman iteration to achieve enhanced output from both systems [31]. Cipolla *et al.* also presented a structure that uses geometric and semantic loss to allow scene analysis with maximum efficiency in multi-task learning [32]. Sun *et al.* developed SegNetMRI as a deep learning technology that reconstructs and segments MRI images using compressed sensing techniques [33]. Sui *et al.* developed RecSeg to incorporate two U-Net structures, making MRI reconstruction faster and lesion segmentation more accurate [34]. Pramanik and Jacob recently employed Deep-SLR to improve the parallel MRI data reconstruction and segmentation function [35].

Recent studies also highlight the use of Electroencephalogram (EEG)-based machine learning models and their application to different neurological disorders with an unmatched accuracy rate [36]. Tripathi *et al.* developed a Weka-based ensemble framework that integrated EEG, Electrocardiogram (ECG), and Electromyography (EMG) signals working with the PhysioNet sleep-bruxism dataset [37]. They reported up to 99% accuracy in detecting sleep bruxism. M.B. Bin Heyat *et al.* [38], which used a Decision Tree classifier with C4–P4 and C4–A1 EEG channels for sleep bruxism detection [39-41]. Wang *et al.* proved that single-channel EEG (C4–P4) and some fine decision tree classifiers could achieve 97.84% accuracy using a small REM-sleep dataset for bruxism detection [42]. In the Attention Deficit Hyperactivity Disorder (ADHD) diagnosis, Saini *et al.* suggested a model to predict ADHD using EEG signals and machine learning methods [43]. This method tested different types of classifiers to improve the accuracy and reliability of the diagnosis of ADHD. The proposed method showed how EEG-based automated systems can help in early identification and can be useful for clinical use. Regarding epilepsy detection, Alalaya *et al.* suggested a method to detect epilepsy using EEG signals [44]. This method used DWT to extract features and then used PCA or t-SNE to reduce the complexity of the data. Several classifiers, such as RF, XGBoost, and MLP, were tested to see which one works best. This method achieved an accuracy of up to 98.98%, which is better than the accuracy reported in previous research.

Table **1** presents a comparative analysis of various deep learning models (CNNs, CNNs with Attention, and Transformers) for classifying Computed Tomography (CT) scans as belonging to a brain tumour [45-50]. It proved that CNNs can be more accurate when used, but they have a variety of limitations, such as capturing the global context or the long-range dependencies. The incorporation of attention-based models enhances feature focus but, at the same time, presents problems such as blurred boundaries and marginal classification errors. Thus, although transformer models seem to be accurate in many tasks, limited data exists comparing them to other techniques for glioma grading or multi-class categorization.

Table 1. A review of deep learning approaches for brain tumour classification.

Author(s)	Methodology	Key Features	Strengths	Remarks
Rasheed *et al.* [11]	CNN	Three-class classification	Efficient feature learning	Baseline CNN; lacks advanced context handling
Abd El-Wahab *et al.* [12]	BTC-FCNN	Fast CNN for MRI	High accuracy, low computation	Prioritizes speed; suited for real-time systems
Ozkaraca *et al.* [13]	Dense CNN	Dense connections	Enhanced feature propagation	Strong feature reuse, but risk of redundancy
Muezzinoglu *et al.* [14]	PatchResNet + KNN	Patch-based deep fusion	Multi-size patch learning	Creative patchwise fusion with classical ML
Mijwil *et al.* [15]	MobileNetV1	Lightweight CNN	Efficient, mobile-friendly	Suitable for edge deployment
Saurav *et al.* [16]	AG-CNN	Attention + GAP	Emphasizes relevant features	Emphasizes spatial attention for classification
Sekhar *et al.* [4]	GoogLeNet + SVM/KNN	Hybrid deep + classical ML	Effective multi-class separation	Combines deep and traditional techniques
Athisayamani *et al.* [17]	ResNet152	Feature extraction + reduction	Strong residual learning	Deep architecture with reduced overfitting
Shahin *et al.* [18]	MBTFCN	Residual + attention	Modular, scalable design	Modular framework with strong potential
Aloraini *et al.* [19]	Transformer + CNN	Hybrid deep learning	Captures long-range dependencies	Innovative mix of CNN and Transformer

(Table 1) contd.....

Author(s)	Methodology	Key Features	Strengths	Remarks
Zulfiqar *et al*. [20]	EfficientNet	Efficient CNN model	High accuracy, low parameters	Balanced accuracy and efficiency
Mehnatkesh *et al*. [21]	ResNet + Ant Colony Optimization	Feature optimization	Intelligent hyperparameter tuning	Uses bio-inspired tuning; novel combo
Singh & Agarwal [22]	CNN for T1WCE	Tailored to specific MRI type	Better domain-specific accuracy	Specialized approach for T1WCE modality
Isunuri & Kakarla [23]	Separable Conv Net	Faster computation	Optimized inference speed	Prioritizes speed with separable convolutions
Raza *et al*. [24]	Deep GoogLeNet (15-layer)	Extended depth	Richer feature extraction	Deep stack model for richer features
Aamir *et al*. [25]	EfficientNet-B0 + Image Segmentation	Contrast enhancement + segmentation	High classification precision	Strong results with preprocessing boost
Wang *et al*. [26]	Full-stack AI	Joint sampling, segmentation	Streamlined MRI workflow	Holistic pipeline from input to diagnosis
Ling *et al*. [27]	MTANet	Multi-task with attention	Strong joint segmentation & classification	Multi-task enhances robustness
Wang *et al*. [28]	MHAN	Multi-stage hybrid attention	Effective feature refinement	Layered attention improves accuracy
Sui *et al*. [29]	ConvNext + multi-task	MRI liver analysis	High accuracy in multi-task setting	Great potential, but for liver MRI
Delannoy *et al*. [30]	SegSRGAN	GAN for segmentation + SR	High-resolution segmentation	Combines SR with accurate segmentation
Corona *et al*. [31]	Nonconvex Bregman Iteration	Joint reconstruction + segmentation	Strong theoretical foundation	Mathematical rigor, practical challenge
Cipolla *et al*. [32]	Multi-task + uncertainty loss	Loss weighting via uncertainty	Efficient scene understanding	Smart uncertainty-based multitasking
Sun *et al*. [33]	SegNetMRI	Unified DL for MRI	Effective joint learning	Specific to compressed sensing
Sui *et al*. [34]	RecSeg (dual U-Net)	Fast MRI + lesion segmentation	Robust to noise, high accuracy	Redundant dual net improves segmentation
Pramanik & Jacob [35]	Deep-SLR	Image domain deep learning	Better parallel MRI handling	Deep learning for fast, quality MRI
Tripathi *et al*. [37]	Ensemble learning using Weka with EEG, ECG, EMG fusion	Power spectral density (EEG), multi-signal fusion, PhysioNet dataset	strong multi-modal approach	Combining EEG with ECG/EMG greatly enhances bruxism detection accuracy
Wang *et al*. [42]	Fine decision tree classifier on single-channel EEG	Time-frequency, nonlinear features, bipolar channels (*e.g.*, C4–P4)	simplicity of single-channel use	Single EEG channel (C4–P4) sufficient for accurate bruxism classification
Saini *et al*. [43]	Applied Naïve Bayes, K-NN, and Logistic Regression on EEG dataset for ADHD prediction	Dataset of 157 children (77 ADHD, 80 healthy), behavioral symptom analysis	K-NN achieved highest accuracy (89%), better than Naïve Bayes and Logistic Regression	Useful for ADHD diagnosis in children
Alalayah *et al*. [44]	DWT for feature extraction, PCA and t-SNE for dimensionality reduction, classifiers: RF, XGBoost, K-NN, DT, MLP	EEG signals, DWT features, PCA + t-SNE, K-means clustering	Achieved 98.98% accuracy using MLP with PCA + K-means, high precision and F1-score	Effective for early epilepsy detection

2. PROPOSED METHODOLOGY

Fig. (**1**) shows the method to classify brain tumours using Magnetic Resonance Imaging scans. Before analysis begins, researchers resize images and eliminate noise by applying a Wiener filter followed by a smoothing process. The Wiener filter enhances image quality by responding to local variations and fighting noise to keep vital edge and texture information that doctors need to diagnose correctly. We normalize and prepare input data before deep learning models perform their processing tasks.

The pre-processed images enter the MPFAN model to dig out functional image content. MPFAN uses multiple processing pathways to examine different kinds of image features at various levels of detail, while attention techniques highlight the most important image areas. The model classifies the images into four categories: The system reacts to MR image input by labelling results into four tumour groups, which include “No Tumour,” “Glioma,” “Pituitary,” and “Meningioma.” The system combines improved processing steps with MPFAN’s focused analysis to help doctors make accurate tumour-type detections.

2.1. Image Preprocessing

Using Wiener filtering enhances medical images accurately, especially when performing vital tasks in medical imaging research [51]. This method lowers image noise to boost overall quality without harming distinct structural and textural parts. Wiener filtering helps prepare MRI images for brain tumour classification before deep learning models can analyze them. The Wiener filter adjusts to image areas to find noise power and then applies ideal smoothing to each region. Compared to standard filters, the Wiener filter keeps vital medical image information intact. It does so by considering both the signal-to-noise ratio and the local variance within the image (Eq. **1**), reducing noise selectively without compromising sharpness.

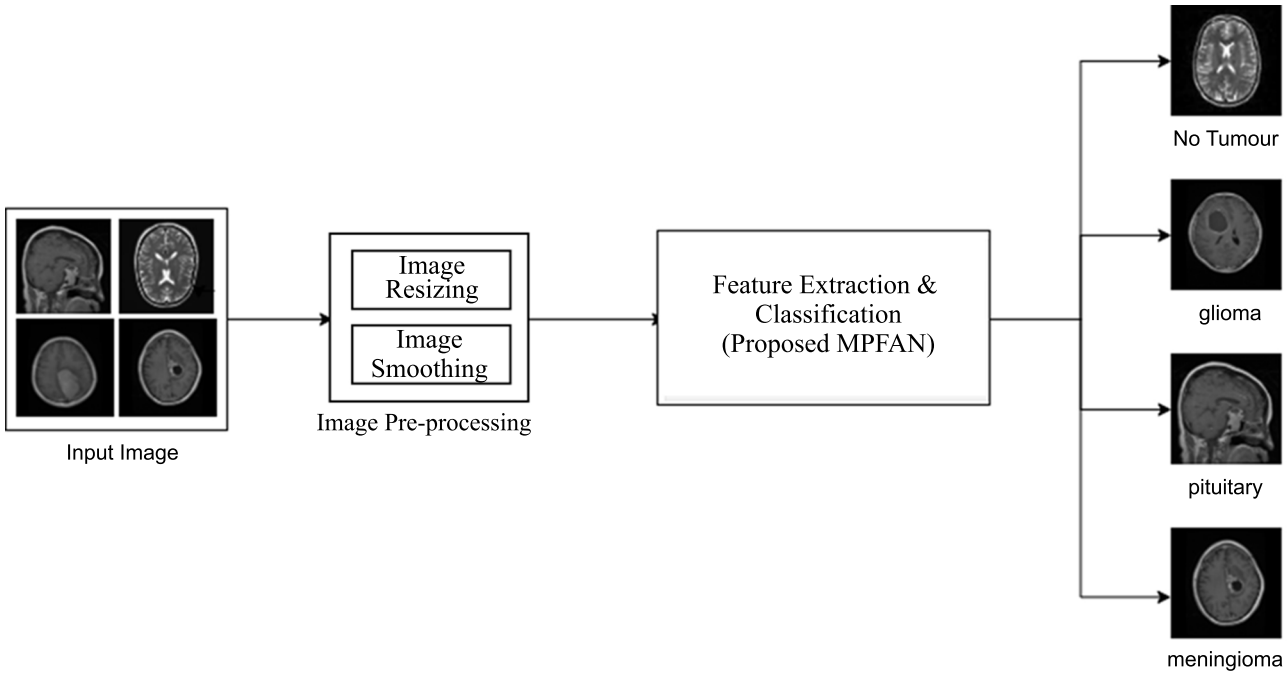

Fig. (1). Workflow of the proposed MPFAN-based brain tumour classification

$$G(u,v) = \frac{H*(u,v)}{|H(u,v)|^2 + \frac{S_{n(u,v)}}{S_{f(u,v)}}} F(u,v) \quad \textbf{(1)}$$

Where G(u,v) is the restored image, H(u,v) represents degradation functions, and F(u,v) is a degraded image in the frequency domain. Here, the power spectral density is represented by $S_{n(u,v)}$ and $S_{f(u,v)}$ for noise and the original image, respectively.

Processing MRI images initially helps remove acquisition noise and environmental interference that may interfere with tumour observation. Wiener filtering both boosts visual contrast and corrects distorted input data to make the results clearer and of better quality. Our deep learning model achieves better detection precision by operating on images that retain natural structure and shape details. The processing system can accurately recognize brain tumours through MRI scans thanks to the Wiener filtering application.

2.2. Proposed Algorithm: Multiscale Parallel Feature Aggregation Network (MPFAN)

A multi-branch convolutional neural network (CNN) architecture incorporating a multiscale feature extraction architecture is proposed to learn multiscale features effectively and achieve robust performance, as shown in Fig. (**2**). It has an input layer of image shape 120 × 120 × 3. The input is processed independently in two parallel branches using convolutional layers (*conv1* and *conv2*) with different kernel sizes and strides. By this configuration, the network can extract different features of the input images. Eqs. **2** and **3**) represent the convolution and max pooling operations that are applied to the images.

$$X' = f(W * X + b) \quad \textbf{(2)}$$

$$X' = max_{(i,j)\in R} X(i,j) \quad \textbf{(3)}$$

Where W, X, and b are kernel, input, and bias, respectively, followed by activation function f(.).

Each branch consists of a series of convolutional blocks, which are then finished with maxpooling layers to decrease spatial measurements while keeping significant hierarchical information. One of the key features of the architecture is the use of concatenation layers, which combine feature maps of different branches. The same is shown in Eq. (**4**), which allows the network to retain and integrate information from multiple scales, preserving global and local spatial patterns.

$$F_{flat} = Concat(features \ldots) \quad \textbf{(4)}$$

To take advantage of the higher accuracy of Thompson sampling on stochastic bandit problems, we propose a multi-branch approach that allows for more complex input data by combining empirical value estimates with Thompson sampling. After the feature extraction process, the network transitions to fully connected layers for high-dimensional transformation and classification. The first step is to flatten the feature maps, transforming the 3D tensors into 1D feature vectors.

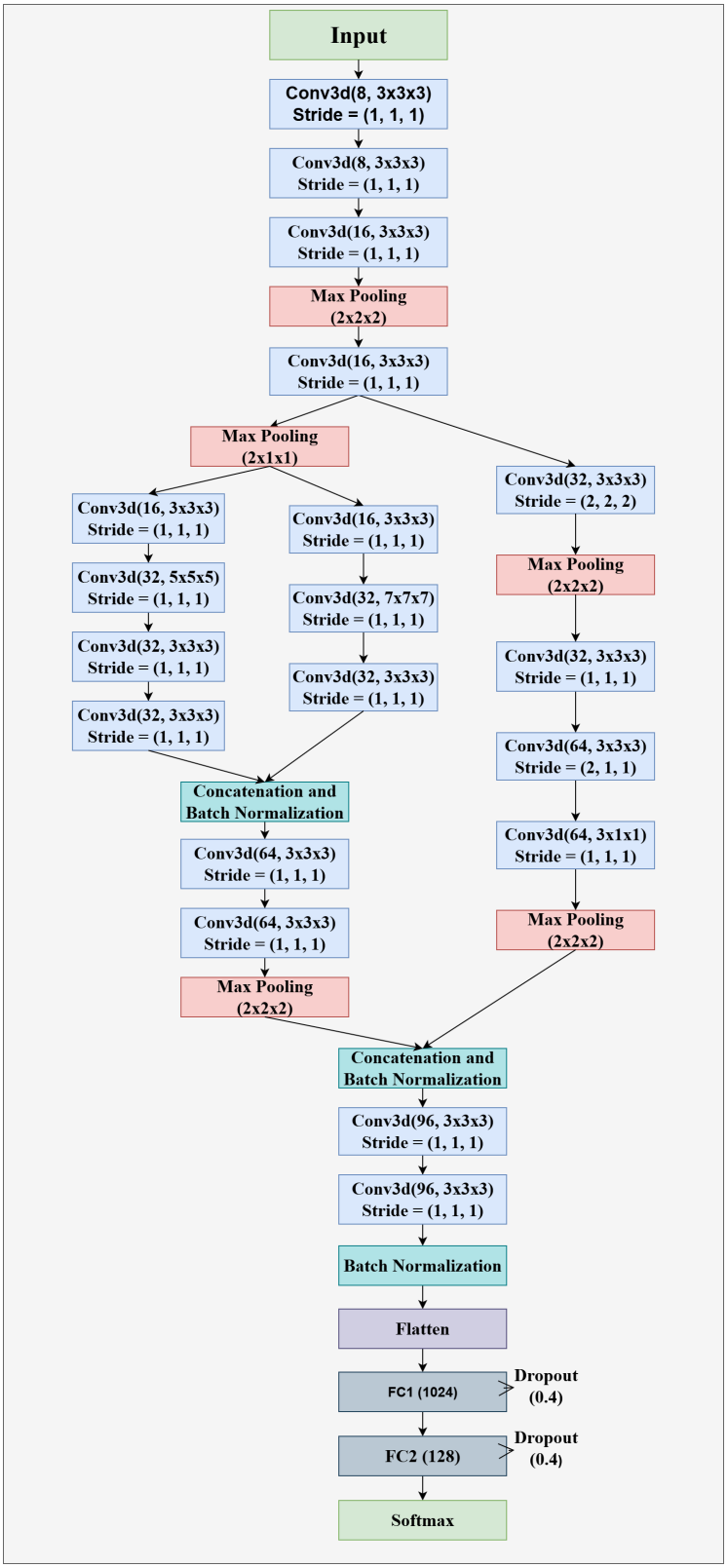

Fig. (2). Architecture of the proposed Multiscale Parallel Feature Aggregation Network (MPFAN).

In the first dense layer, we set the number of neurons to 2048 to learn complex patterns (beyond simple lines and planes) in the data. These learned features are passed through a second dense layer with 512 neurons for further refinement. To prevent the model from overfitting, dropout layers with well-chosen rates are applied after each dense layer to ensure that the model generalizes well to unseen data. Depending on whether the task is binary classification, the final dense layer consists of a single neuron with either a linear or sigmoid activation function. Eq. (**5**) shows the functionality of a fully connected layer, and softmax classification is represented by Eq. (**6**).

$$FC = f(W_{fc} \cdot F_{flat} + b_{fc}) \quad \textbf{(5)}$$

$$P(y_i) = \frac{e^{z_i}}{\sum_j e^{z_j}} \quad \textbf{(6)}$$

With its multi-branch design, layered structure, feature concatenation, and regularization techniques, the network is naturally suited for tasks that require high-dimensional input processing and precise feature extraction and classification.

2.3. Pseudo Code for MPFAN

Our MPFAN model implementation starts by defining the size of the MRI image inputs. The input layer processes the images and passes them through two separate convolutional branches: one with a smaller filter size. Our design uses one convolutional branch with 3 × 3 filters and another with 5 × 5 filters. These layers shrink feature maps by taking their maximum values during each subsampling step. The model merges scale feature maps from each input branch to build its overall representation.

A layer of 2048 neurons with ReLU activation builds complex features that reduce the dropout layer with 0.4 probability to prevent overfitting. After processing through 512 neurons, the layer refines another step-in feature extraction before traditional dropout protection. The model's final layer consists of one neuron with a sigmoid activation to provide tumour malignancy likelihood. The model trains best using Adam optimization and binary cross-entropy loss to achieve proper results. The same has been presented as an algorithm in Algorithm 1 for the proposed MPFAN model.

Algorithm 1: Multiscale Parallel Feature Aggregation Network (MPFAN)

1: **Input:** MRI brain image $I \in R120\times120\times3$

2: **Output:** Tumour classification $y \in \{Glioma, Meningioma, Pituitary, No\ Tumour\}$

3: Load MRI brain tumour image of size 120 × 120 × 3.

4: $F_{A1} \leftarrow \text{ReLU}(\text{Conv2D}_{32,3\times3,s=2}(I))$

5: $F_{A2} \leftarrow \text{ReLU}(\text{Conv2D}_{32,3\times3,s=1}(F_{A1}))$

6: $F_{A3} \leftarrow \text{ReLU}(\text{Conv2D}_{64,3\times3,s=1}(F_{A2}))$

7: $P_A \leftarrow \text{MaxPool}_{3\times3}(F_{A3})$

8: $P_{A''} \leftarrow \text{ReLU}(\text{Conv2D}_{64,3\times3,s=2}(F_{A3}))$

9: Concatenate: $F_1 \leftarrow \text{Concat}(P_A, P_{A''})$

10: $F_{C1} \leftarrow \text{ReLU}(\text{Conv2D}_{64,1\times1,s=1}(F_1))$

11: $F_{C2} \leftarrow \text{ReLU}(\text{Conv2D}_{64,5\times1,s=1}(F_{C1}))$

12: $F_{C3} \leftarrow \text{ReLU}(\text{Conv2D}_{64,1\times5,s=1}(F_{C2}))$

13: $F_{C4} \leftarrow \text{ReLU}(\text{Conv2D}_{96,3\times3,s=1}(F_{C3}))$

14: $F_{D1} \leftarrow \text{ReLU}(\text{Conv2D}_{64,3\times3,s=1}(F_1))$

15: $F_{D2} \leftarrow \text{ReLU}(\text{Conv2D}_{96,5\times5,s=1}(F_{D1}))$

16: Concatenate: $F_2 \leftarrow \text{Concat}(F_{C4}, F_{D2})$

17: $P_{F2} \leftarrow \text{MaxPool}_{3\times3}(F_2)$

18: $F_{E1} \leftarrow \text{ReLU}(\text{Conv2D}_{96,3\times3,s=1}(F_2))$

19: Concatenate: $F_3 \leftarrow \text{Concat}(P_{F2}, F_{E1})$

20: $F_{B1} \leftarrow \text{ReLU}(\text{Conv2D}_{64,1\times1,s=2}(I))$

21: $F_{B2} \leftarrow \text{ReLU}(\text{Conv2D}_{64,3\times1,s=1}(F_{B1}))$

22: $F_{B3} \leftarrow \text{ReLU}(\text{Conv2D}_{64,1\times3,s=1}(F_{B2}))$

23: $P_{FB3} \leftarrow \text{MaxPool}_{3\times3}(F_{B3})$

24: $F_{E1} \leftarrow \text{ReLU}(\text{Conv2D}_{64,1\times1,s=1}(P_{FB3}))$

25: $F_{E2} \leftarrow \text{ReLU}(\text{Conv2D}_{64,5\times1,s=1}(F_{E1}))$

26: $F_{E3} \leftarrow \text{ReLU}(\text{Conv2D}_{96,1\times5,s=1}(F_{E2}))$

27: $F_{E4} \leftarrow \text{ReLU}(\text{Conv2D}_{96,1\times1,s=2\times1}(F_{E3}))$

28: $F_{E5} \leftarrow \text{ReLU}(\text{Conv2D}_{96,3\times3,s=1}(F_{E4}))$

29: $P_{FE5} \leftarrow \text{MaxPool}_{3\times3}(F_{E5})$

30: Concatenate: $F_4 \leftarrow \text{Concat}(P_{FE5}, F_3)$

31: $P_3 \leftarrow \text{MaxPool}_{3\times3}(F_4)$

32: Flatten the pooled feature map: $F_f \leftarrow \text{Flatten}(P_3)$

33: Fully connected layer 1: $h_1 \leftarrow \text{ReLU}(W_1F_f + b_1)$, then apply Dropout ($p = 0.4$)

34: Fully connected layer 2: $h_2 \leftarrow \text{ReLU}(W_2h_1 + b_2)$, then apply Dropout ($p = 0.4$)

35: Final output: $\hat{y} \leftarrow \text{Softmax}(W_3h_2 + b_3)$

36: Predicted class: $y \leftarrow \text{Argmax}(\hat{y})$

The algorithm is run on an MRI dataset with 32 images per batch during 100 training rounds. We use labeled MRI images to train our model and validate performance by checking results with the validation data. The MPFAN model achieves good results while also running efficiently for brain tumour diagnosis tasks.

2.4. Dataset Description

The Brain Tumour MRI Dataset provides a comprehensive collection of MRI scans for brain tumour classification [52, 53]. It includes four tumour categories: Gliomas (300 images), Meningiomas (306 images), Pituitary Tumours (300 images), and No Tumours (405 images). This dataset is well-suited for deep learning applications focused on automatic tumour detection and classification.

Table 2. Performance analysis of the proposed method for different epochs.

Epoch	TA	TL	TP	TR	TF	VA	VL	VP	VR	VF
20	0.956	0.092	0.958	0.956	0.951	0.961	0.082	0.962	0.961	0.957
40	0.975	0.069	0.976	0.974	0.971	0.975	0.064	0.975	0.975	0.973
60	0.983	0.055	0.983	0.982	0.98	0.986	0.057	0.987	0.984	0.98
80	0.984	0.055	0.985	0.984	0.983	0.964	0.078	0.966	0.964	0.958
100	0.985	0.053	0.985	0.985	0.983	0.974	0.072	0.977	0.974	0.974

Note: *T=Training, V=Validation, A=Accuracy, L=Loss, P=Precision, R=Recall, F=F1-Measure.

Table 3. Comparative analysis of proposed approach for different optimizers.

Optimizer	TA	TL	TP	TR	TF	VA	VL	VP	VR	VF
RMS Prop	0.922	0.129	0.93	0.919	0.918	0.887	0.195	0.894	0.878	0.869
Ada-Delta	0.99	0.042	0.991	0.99	0.989	0.972	0.071	0.977	0.972	0.97
Adam	0.985	0.053	0.985	0.985	0.983	0.974	0.072	0.977	0.974	0.974
SGD	0.987	0.05	0.988	0.987	0.986	0.958	0.113	0.959	0.958	0.953
AdaGrad	0.98	0.058	0.98	0.979	0.975	0.964	0.078	0.966	0.963	0.96

Given the challenges of low-quality imaging and undersampled data, our MPFAN model addresses these issues by extracting multiscale features and processing them in parallel. The dataset is used for both training and performance evaluation of the MPFAN model, with key aspects including multiscale feature extraction to capture tumour characteristics at different spatial levels, parallel processing for improved feature representation, and classification accuracy, efficiency, and feature robustness as the primary performance metrics.

3. RESULTS AND DISCUSSION

The comparative analysis of different epochs indicates a consistent improvement in performance metrics over time, as shown in Table **2**. Validation and training accuracy increase as the model trains from 20 to 100 epochs. At epoch 100, the validation accuracy hits 0.974 while training accuracy reaches 0.985. As the model trains over time, its optimization improves, resulting in lower training (0.053) and validation loss (0.072). The changes in TR and TF results ensure better model performance, while TP gains show steady progress in reliability. Our results show signs of overfitting from validation metrics in later epoch updates. Our findings show that increasing model training time produces better results yet requires manual optimization to maintain prediction reliability.

The analysis finds that Ada-Delta is the most effective optimizer because it delivers top accuracy (0.990) and validation accuracy (0.972) across all performance measures. In Table **3**, Adam’s superior performance shows that this optimizer produces 0.985 top accuracy and 0.974 validation accuracy. Gradient Descent proves itself through a Test Accuracy (0.987) that is slightly lower than its Validation Accuracy (0.958). In performance testing, AdaGrad generates acceptable results with accuracy scores of 0.980 for training and 0.964 for validation. RMS Prop ranks lowest among tested optimizers because it achieves a TA of 0.922 and a VA of 0.887 compared to other optimization methods.

As illustrated in Fig. (**3**), the trade-off curves capturing the model's learning dynamics on brain tumor classification showcase the trade-offs between accuracy, loss, precision, recall, and F1-score. Inaccuracy measurement subsection (Fig. **3a**), training accuracy appears to improve throughout epochs and levels off at around 98.5% while validation accuracy plateaus slightly below at about 97.4%. This indicates strong model generalization with negligible overfitting issues. Validation loss presented in slice (Fig. **3b**) demonstrates trends linking cross-entropy losses for both datasets, whereby training loss decreases to a value of 0.053 and validation loss settles just under 0.072, confirming effective convergence without underfitting issues persisting. These observations support claims regarding high optimisation efficiency provided by applying the Adam algorithm, as well as confirming that the model acquires proper representations during the training phase, unexposed to excessive overfitting or underfitting during alternating training and validating stages.

The model's classification performance is further analyzed and highlighted in training and validation using precision, recall, and F1-score curves shown in subfigures (Fig. **3c**-**e**). The training precision peaks at 98.5% while validation precision stabilizes around 97.7%, reinforcing the claim that false positives are minimized. Also, recall values, which indicate a model's sensitivity, hit 98.5% for training and 97.4% for validation, which means almost all true tumor cases are captured. The F1-score captures both precision and recall, achieving 98.3% on the training set while validation yields 97.4%. Having strong results across the board reflects the classification ability of the model.

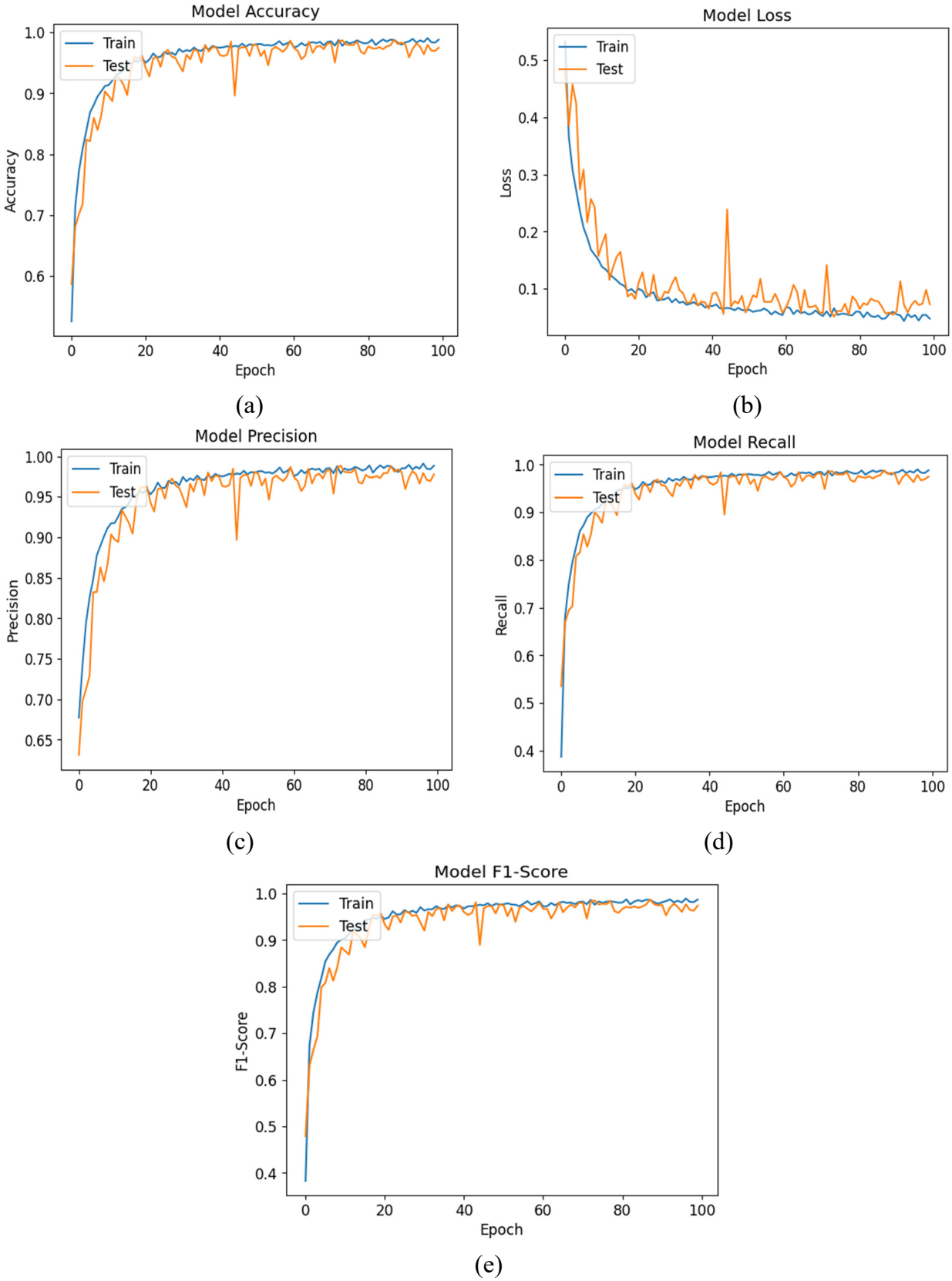

Fig. (3). Trade-off curves between training and validation (a) Accuracies, (b) Loss, (c) Precision, (d) Recall, (e) F1-Score

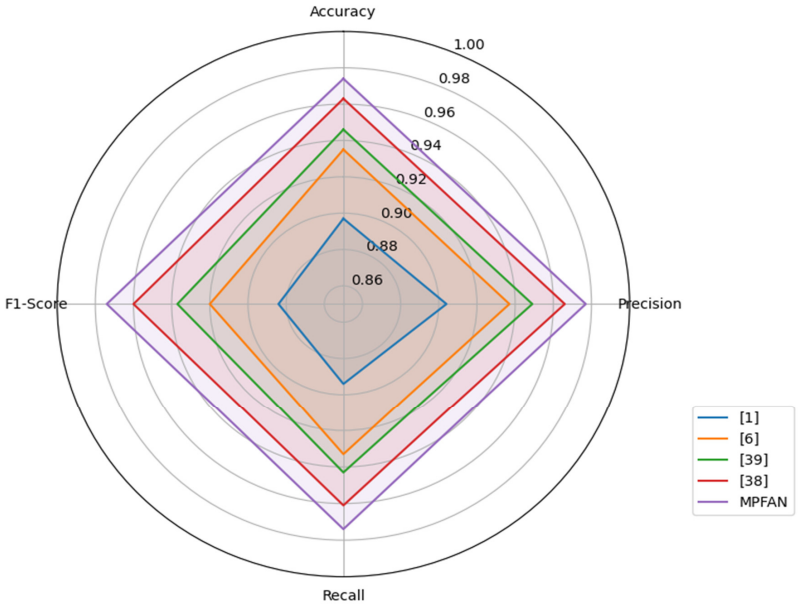

Fig. (4). Comparison with Existing Methods.

The close distance of these metrics across training and validation illustrates the strength of the model, alongside its stability over epochs, suggesting strong overall performance even with multilabel medical images from diverse domains within healthcare fields spanning many specialties. All together, these confirm that the accuracy estimations reached by the proposed model for real-time detection of brain tumors in support systems are trustworthy.

3.1. Comparison with Existing State-of-the-Art

This study compares MPFAN against leading brain tumour classification techniques that exist today, as found in Fig. (**4**). The MPFAN system delivers outstanding performance in every metric, with a precision of 0.977 and outcomes that closely match each other. MPFAN performs better than competing systems, which reported 0.963 accuracy and 0.960 F1 measure data. Our study shows that breaking up tumour features at multiple scales and then analyzing them together improves detection accuracy to establish a new classification benchmark.

3.2. Ablation Study

We have performed an extensive ablation study to understand the contribution of each architectural component of the proposed MPFAN model. Here, we have tested the performance impact of removing or modifying important components such as the multi-branch structure, feature fusion strategy, dropout regularization, optimizer, and dense layer configuration. Table **4** presents the results of the comparative analysis of each architectural component of MPFAN. The baseline MPFAN model achieved a classification accuracy of 97.4% on the brain tumor MRI dataset. Removing one of the parallel branches (3×3 or 5×5 convolution) caused a drop in accuracy to 93.1%, underscoring the importance of extracting multiscale features. Additionally, using the same kernel size in both branches, accuracy dropped to 94.5%, suggesting that capturing rich spatial features requires multiple receptive fields.

Table 4. Comparative evaluation of MPFAN with different architectural ablation variants.

Description	Accuracy (%)	Drop in Accuracy w.r.t. MPFAN
Proposed Method (MPFAN)	97.4	-
Remove one parallel branch (use only 3×3 conv)	93.1	↓ 4.3
Use same kernel size in both branches (3×3 for both)	94.5	↓ 2.9
Remove feature concatenation (keep outputs separate)	91.8	↓ 5.6
Remove dropout layers	95.2	↓ 2.2
Reduce dense layer size (1024 → 256 instead of 2048 → 512)	94.7	↓ 2.7
Replace Adam with SGD optimizer	95.8	↓ 1.6
Remove max pooling in branches	92.5	↓ 4.9
Single-scale CNN (no multiscale branches)	90.4	↓ 7.0

Moreover, eliminating the concatenation of features also resulted in a notable accuracy drop to 91.8%, underscoring its vital role in maintaining multiscale spatial quantitative information. The removal of dropout also reduced accuracy to 95.2%, confirming the regularization effect of dropout, which is clearly necessary in avoiding overfitting.

The accuracy is dropped to 2% (*i.e.*, 94.7%) with the modification changing dense layers from 2048→512 to 1024→256. This shows a need for greater feature transformation ability in the classification phase. Changing the optimizer from Adam to SGD caused a slight drop to 95.8%, suggesting better convergence properties of Adam for this architecture. Also, removing max pooling in the branches or using a single-scale CNN (no multi-branch structure) caused a significant loss in performance, down to 92.5% and 90.4%, respectively. These results support the design choices made in the MPFAN and illustrate the need for multiscale processing in parallel with hierarchical feature integration to achieve precise brain tumor classification.

3.3. Constraints of the Study

Results aside from the strong performance of the proposed MPFAN model in brain tumor classification, MPFAN shows several limitations that may most likely impact interpretation and generalization. The model is trained and validated using a single benchmark MRI dataset, which does not consider the variability present in real-world clinical scenarios with different imaging devices, patient demographics, and scanning protocols.

Moreover, the model demonstrated high accuracy across epochs and optimizers; however, signs of overfitting at the later stages of training indicate that there could be a sensitivity to performance related to the training duration and the hyperparameter settings. Furthermore, the fixed choices of parameters, like the optimizer and the architectural designs used, may pose barriers to reproducibility and scalability without some form of automated optimization. Although the ablation study validated that every architecture component is important, the study did not address the robustness of MPFAN under noise in the data or incomplete information, which tend to be more prevalent in clinical settings. Such shortcomings need to be addressed in subsequent work to improve the model’s clinical relevance and potential for widespread use.

4. CONCLUSION AND FUTURE DIRECTIONS

The MPFAN (Multiscale Parallel Feature Aggregation Network) model is developed to improve brain tumor detection by parallel feature extraction at multiple scales. MPFAN can capture fine-grained local and global contextual patterns in MRI brain scans with its multi-branch convolutional architecture and hierarchically integrated feature fusion approach. MPFAN overcomes challenges like feature redundancy, insufficient multiscale pattern representation, and poor computation efficiency in traditional CNN models by concurrently processing image data from varying receptive fields, effectively integrating them. This marks a stark difference from our model, which, while still being resource considerate, enables low-resource demand environments like clinical settings to leverage the model in real-time.

As for work to tackle in the future, we intend to optimize MPFAN by adding an Attention Fusion Network to supersede conventional concatenation layers. This will allow the network to selectively concentrate on the most important feature maps during training and inference processes, making the model achieve these tasks much faster, reducing overfitting, and lowering model complexity. Moreover, we plan to add residual connections and bottleneck structures to strengthen the gradient flow and improve convergence and generalization performance. For future research, we want to modify the architecture of MPFAN for use in multimodal medical imaging, like combining MRI with PET or CT scans, while also broadening its use to include the classification of various neurological and oncological abnormalities. Moreover, the explainability modules, such as Grad-CAM or SHAP, may be examined to enhance clinical trust and provide insight into the network's reasoning. With such enhancements, the MPFAN can develop into a strong, flexible architecture for a complete analysis of medical images.

AUTHORS’ CONTRIBUTIONS

The authors confirm their contribution to the paper as follows: M.A.A., A.M.: Conceptualization; B.D.S.: Data analysis or interpretation; S.A., P.S., M.D., S.A.: Draft manuscript. All authors reviewed the results and approved the final version of the manuscript.

LIST OF ABBREVIATIONS

MPFAN	=	Multiscale Parallel Feature Aggregation Network
MRI	=	Magnetic resonance imaging
CNN	=	Convolutional Neural Network
SVM	=	Support Vector Machine
KNN	=	K-Nearest Neighbour
AG-CNN	=	Attention-Guided Convolutional Neural Network
GAP	=	Global Average Pooling
BTC-FCNN	=	Brain Tumour Classification-Fast Convolutional Neural Network
MBTFCN	=	Modular Brain Tumour Fully Convolutional Network
MTANet	=	Multi-task Attention Network
MHAN	=	Multi-stage Hybrid Attention Network
GAN	=	Generative Adversarial Network,
EEG	=	Electroencephalogram
ECG	=	Electrocardiogram
EMG	=	Electromyography
DWT	=	Discrete Wavelet Transform
ADHD	=	Attention Deficit Hyperactivity Disorder
SGD	=	Stochastic Gradient Descent
ReLU	=	Rectified Linear Unit.

ETHICS APPROVAL AND CONSENT TO PARTICIPATE

Not applicable.

HUMAN AND ANIMAL RIGHTS

Not applicable.

CONSENT FOR PUBLICATION

Not applicable.

AVAILABILITY OF DATA AND MATERIAL

The data supporting the findings of the article is available in the Kaggle repository at https://www.kaggle.com/datasets/masoudnickparvar/brain-tumor-mri-dataset, reference number [53].

CONFLICT OF INTEREST

Dr. Salman Akhtar is the Associate Editorial Board Member of The Open Bioinformatics Journal.

FUNDING

None.

ACKNOWLEDGEMENTS

declared none.

REFERENCES

[1] Samreen A, Taha A, Reddy Y, Sathish P. Brain tumor detection by using convolution neural network. Int J Online Biomed Eng 2020; 16(13): 58-69. http://dx.doi.org/10.3991/ijoe.v16i13.18545

[2] Amin J, Sharif M, Haldorai A, Yasmin M, Nayak RS. Brain tumor detection and classification using machine learning: A comprehensive survey. Complex Intell Syst 2022; 8(4): 3161-83. http://dx.doi.org/10.1007/s40747-021-00563-y

[3] Chandni , Sachdeva M, Kushwaha AKS. AI-based intelligent hybrid framework (BO-DenseXGB) for multi- classification of brain tumor using MRI. Image Vis Comput 2025; 154: 105417. http://dx.doi.org/10.1016/j.imavis.2025.105417

[4] Sekhar A, Biswas S, Hazra R, Sunaniya AK, Mukherjee A, Yang L. Brain tumor classification using fine-tuned GoogLeNet features and machine learning algorithms: IoMT enabled CAD system. IEEE J Biomed Health Inform 2022; 26(3): 983-91. http://dx.doi.org/10.1109/JBHI.2021.3100758 PMID: 34324425

[5] Barman B, Dewang RK, Mewada A. Facial recognition using grey wolf optimization. Mater Today Proc 2022; 58: 273-85. http://dx.doi.org/10.1016/j.matpr.2022.02.161

[6] Tiwari M, Singh N, Mewada A, Ansari MA. Machine learning empowered breast cancer diagnosis: Insights from Coimbra dataset. Recent Adv Comput Sci Commun 2024; 18(3) http://dx.doi.org/10.2174/0126662558297605240926055723

[7] Wu Z, Liao W, Yan C, *et al*. Deep learning based MRI reconstruction with transformer. Comput Methods Programs Biomed 2023; 233: 107452. http://dx.doi.org/10.1016/j.cmpb.2023.107452 PMID: 36924533

[8] Liu Y, Pang Y, Liu X, Liu Y, Nie J. DIIK-Net: A full-resolution cross-domain deep interaction convolutional neural network for MR image reconstruction. Neurocomputing 2023; 517: 213-22. http://dx.doi.org/10.1016/j.neucom.2022.09.048

[9] Wang Y, Pang Y, Tong C. DSMENet: Detail and structure mutually enhancing network for under-sampled MRI reconstruction. Comput Biol Med 2023; 154: 106204. http://dx.doi.org/10.1016/j.compbiomed.2022.106204 PMID: 36716684

[10] Wang S, Wu J, Chen M, Huang S, Huang Q. Balanced transformer: efficient classification of glioblastoma and primary central nervous system lymphoma. Phys Med Biol 2024; 69(4): 045032. http://dx.doi.org/10.1088/1361-6560/ad1f88 PMID: 38232389

[11] Rasheed Z, Ma YK, Ullah I, *et al*. Automated classification of brain tumors from magnetic resonance imaging using deep learning. Brain Sci 2023; 13(4): 602. http://dx.doi.org/10.3390/brainsci13040602 PMID: 37190567

[12] Abd El-Wahab BS, Nasr ME, Khamis S, Ashour AS. BTC-FCNN: Fast convolution neural network for multi-class brain tumor classification. Health Inf Sci Syst 2023; 11(1): 3. http://dx.doi.org/10.1007/s13755-022-00203-w PMID: 36606077

[13] Özkaraca O, Bağrıaçık Oİ, Gürüler H, *et al*. Multiple brain tumor classification with dense CNN architecture using brain MRI images. Life 2023; 13(2): 349. http://dx.doi.org/10.3390/life13020349 PMID: 36836705

[14] Muezzinoglu T, Baygin N, Tuncer I, *et al*. PatchResNet: Multiple patch division–based deep feature fusion framework for brain tumor classification using MRI images. J Digit Imaging 2023; 36(3): 973-87. http://dx.doi.org/10.1007/s10278-023-00789-x PMID: 36797543

[15] Mijwil MM, Doshi R, Hiran KK, Unogwu OJ, Bala I. MobileNetV1-based deep learning model for accurate brain tumor classification. Mesopotamian J Comput Sci 2023; 29-38. http://dx.doi.org/10.58496/MJCSC/2023/005

[16] Saurav S, Sharma A, Saini R, Singh S. An attention-guided convolutional neural network for automated classification of brain tumor from MRI. Neural Comput Appl 2023; 35(3): 2541-60. http://dx.doi.org/10.1007/s00521-022-07742-z

[17] Athisayamani S, Antonyswamy RS, Sarveshwaran V, Almeshari M, Alzamil Y, Ravi V. Feature extraction using a residual deep convolutional neural network (ResNet-152) and optimized feature dimension reduction for MRI brain tumor classification. Diagnostics 2023; 13(4): 668. http://dx.doi.org/10.3390/diagnostics13040668 PMID: 36832156

[18] Shahin AI, Aly W, Aly S. MBTFCN: A novel modular fully convolutional network for MRI brain tumor multi-classification. Expert Syst Appl 2023; 212: 118776. http://dx.doi.org/10.1016/j.eswa.2022.118776

[19] Aloraini M, Khan A, Aladhadh S, Habib S, Alsharekh MF, Islam M. Combining the transformer and convolution for effective brain tumor classification using MRI images. Appl Sci 2023; 13(6): 3680. http://dx.doi.org/10.3390/app13063680

[20] Zulfiqar F, Ijaz Bajwa U, Mehmood Y. Multi-class classification of brain tumor types from MR images using EfficientNets. Biomed Signal Process Control 2023; 84: 104777. http://dx.doi.org/10.1016/j.bspc.2023.104777

[21] Mehnatkesh H, Jalali SMJ, Khosravi A, Nahavandi S. An intelligent driven deep residual learning framework for brain tumor classification using MRI images. Expert Syst Appl 2023; 213: 119087. http://dx.doi.org/10.1016/j.eswa.2022.119087

[22] Singh R, Agarwal BB. An automated brain tumor classification in MR images using an enhanced convolutional neural network. Int J Inf Technol 2023; 15(2): 665-74. http://dx.doi.org/10.1007/s41870-022-01095-5

[23] Isunuri BV, Kakarla J. Three-class brain tumor classification from magnetic resonance images using separable convolution based neural network. Concurr Comput 2022; 34(1): e6541. http://dx.doi.org/10.1002/cpe.6541

[24] Raza A, Ayub H, Khan JA, *et al*. A hybrid deep learning-based approach for brain tumor classification. Electronics 2022; 11(7): 1146. http://dx.doi.org/10.3390/electronics11071146

[25] Aamir M, Rahman Z, Dayo ZA, *et al*. A deep learning approach for brain tumor classification using MRI images. Comput Electr Eng 2022; 101: 108105. http://dx.doi.org/10.1016/j.compeleceng.2022.108105

[26] Wang Z, Li B, Yu H, *et al*. Promoting fast MR imaging pipeline by

full-stack AI. iScience 2024; 27(1): 108608.
http://dx.doi.org/10.1016/j.isci.2023.108608 PMID: 38174317

[27] Ling Y, Wang Y, Dai W, Yu J, Liang P, Kong D. MTANet: Multi-task attention network for automatic medical image segmentation and classification. IEEE Trans Med Imaging 2024; 43(2): 674-85.
http://dx.doi.org/10.1109/TMI.2023.3317088 PMID: 37725719

[28] Wang W, Shen H, Chen J, Xing F. MHAN: Multi-stage hybrid attention network for MRI reconstruction and super-resolution. Comput Biol Med 2023; 163: 107181.
http://dx.doi.org/10.1016/j.compbiomed.2023.107181 PMID: 37352637

[29] Sui D, Liu W, Guo M, *et al*. Flexible ConvNeXt block based multi-task learning framework for liver MRI images analysis. 2022 IEEE International Conference on Bioinformatics and Biomedicine (BIBM). Las Vegas, NV, USA, 2019, pp. 2119-2126.
http://dx.doi.org/10.1109/BIBM55620.2022.9994956

[30] Delannoy Q, Pham CH, Cazorla C, *et al*. SegSRGAN: Super-resolution and segmentation using generative adversarial networks: Application to neonatal brain MRI. Comput Biol Med 2020; 120: 103755.
http://dx.doi.org/10.1016/j.compbiomed.2020.103755 PMID: 32421654

[31] Corona V, Benning M, Ehrhardt MJ, *et al*. Enhancing joint reconstruction and segmentation with non-convex Bregman iteration. Inverse Probl 2019; 35(5): 055001.
http://dx.doi.org/10.1088/1361-6420/ab0b77

[32] Cipolla R, Gal Y, Kendall A. Multi-task learning using uncertainty to weigh losses for scene geometry and semantics. IEEE/CVF Conference on Computer Vision and Pattern Recognition (CVPR). Salt Lake City, UT, USA, 2018, pp. 7482-7491.
http://dx.doi.org/10.1109/CVPR.2018.00781

[33] Sun L, Fan Z, Ding X, Huang Y, Paisley J. Joint CS-MRI reconstruction and segmentation with a unified deep network. Information Processing in Medical Imaging. IPIM 2019; pp. 492-504.
http://dx.doi.org/10.1007/978-3-030-20351-1_38

[34] Sui B, Lv J, Tong X, Li Y, Wang C. Simultaneous image reconstruction and lesion segmentation in accelerated MRI using multitasking learning. Med Phys 2021; 48(11): 7189-98.
http://dx.doi.org/10.1002/mp.15213 PMID: 34542180

[35] Pramanik A, Jacob M. Reconstruction and segmentation of parallel MR data using image domain Deep-SLR. 2021 IEEE 18th International Symposium on Biomedical Imaging (ISBI). Nice, France, 13-16 April 2021.
http://dx.doi.org/10.1109/ISBI48211.2021.9434056

[36] Iqbal MS, Belal Bin Heyat M, Parveen S, *et al*. Progress and trends in neurological disorders research based on deep learning. Comput Med Imaging Graph 2024; 116: 102400.
http://dx.doi.org/10.1016/j.compmedimag.2024.102400 PMID: 38851079

[37] Tripathi P, Ansari MA, Gandhi TK, Albalwy F, Mehrotra R, Mishra D. Computational ensemble expert system classification for the recognition of bruxism using physiological signals. Heliyon 2024; 10(4): e25958.
http://dx.doi.org/10.1016/j.heliyon.2024.e25958 PMID: 38390100

[38] Heyat MBB, Lai D, Khan FI, Zhang Y. Sleep bruxism detection using decision tree method by the combination of C4-P4 and C4-A1 channels of scalp EEG. IEEE Access 2019; 7: 102542-53.
http://dx.doi.org/10.1109/ACCESS.2019.2928020

[39] Heyat MBB, Akhtar F, Khan MH, *et al*. Detection, treatment planning, and genetic predisposition of bruxism: A systematic mapping process and network visualization technique. CNS Neurol Disord Drug Targets 2021; 20(8): 755-75.
http://dx.doi.org/10.2174/19963181MTExyMzM33 PMID: 33172381

[40] Bin Heyat MB, Lai D, Wu K, *et al*. Role of oxidative stress and inflammation in insomnia sleep disorder and cardiovascular diseases: Herbal antioxidants and anti-inflammatory coupled with insomnia detection using machine learning. Curr Pharm Des 2022; 28(45): 3618-36.
http://dx.doi.org/10.2174/1381612829666221201161636 PMID: 36464881

[41] Heyat MBB, Akhtar F, Munir F, *et al*. Unravelling the complexities of depression with medical intelligence: exploring the interplay of genetics, hormones, and brain function. Complex Intell Syst 2024; 10(4): 5883-915.
http://dx.doi.org/10.1007/s40747-024-01346-x

[42] Wang C, Verma AK, Guragain B, Xiong X, Liu C. Classification of bruxism based on time-frequency and nonlinear features of single channel EEG. BMC Oral Health 2024; 24(1): 81.
http://dx.doi.org/10.1186/s12903-024-03865-y PMID: 38221633

[43] Saini S, Rani R, Kalra N. Prediction of attention deficit hyperactivity disorder (ADHD) using machine learning techniques based on classification of EEG signal. 2022 8th International Conference on Advanced Computing and Communication Systems (ICACCS). Coimbatore, India, 25-26 March 2022.

[44] Alalayah KM, Senan EM, Atlam HF, Ahmed IA, Shatnawi HSA. Effective early detection of epileptic seizures through EEG signals using classification algorithms based on t-distributed stochastic neighbor embedding and K-means. Diagnostics 2023; 13(11): 1957.
http://dx.doi.org/10.3390/diagnostics13111957 PMID: 37296809

[45] Ahmad S, Hussain S, Anwar K, Verma H, Sharma D, Aggarwal A. Exploring the landscape of cloud robotics: A comprehensive review. 2024 15th International Conference on Computing Communication and Networking Technologies (ICCCNT). Kamand, India, 24-28 June 2024.
http://dx.doi.org/10.1109/ICCCNT61001.2024.10724868

[46] Vinod DS, Prakash SPS, AlSalman H, Muaad AY, Heyat MBB. Ensemble technique for brain tumor patient survival prediction. IEEE Access 2024; 12: 19285-98.
http://dx.doi.org/10.1109/ACCESS.2024.3360086 ; Mehrotra R, Ansari MA, Agrawal R, *et al*. Deep convolutional network-based probabilistic selection approach for multiclassification of brain tumors using magnetic resonance imaging. Int J Intell Syst 2025; 2025(1): 6914757.
http://dx.doi.org/10.1155/int/6914757

[47] Bin Heyat MB, Akhtar F, Abbas SJ, *et al*. Wearable flexible electronics based cardiac electrode for researcher mental stress detection system using machine learning models on single lead electrocardiogram signal. Biosensors 2022; 12(6): 427.
http://dx.doi.org/10.3390/bios12060427 PMID: 35735574

[48] Mewada A, Maurya SK, Ansari MA. Seeing beyond: Advanced image and thermal analysis for early detection of diabetic retinopathy and diabetes. Biomed Pharmacol J 2025; 18: 191-202.
http://dx.doi.org/10.13005/bpj/3081

[49] Muaad AY, Raza S, Heyat MBB, Alabrah A, J H. An intelligent COVID-19-related Arabic text detection framework based on transfer learning using context representation. Int J Intell Syst 2024; 2024(1): 1-15.
http://dx.doi.org/10.1155/2024/8014111

[50] Kousar F, Sultana A, Albahar MA, *et al*. A cross-sectional study of parental perspectives on children about COVID-19 and classification using machine learning models. Front Public Health 2025; 12: 1373883.
http://dx.doi.org/10.3389/fpubh.2024.1373883 PMID: 39882116

[51] Ansari MA, Kurchaniya D, Dixit M. A comprehensive analysis of image edge detection techniques. International J Mult Ubiquit Eng 2017; 12(11): 1-12.
http://dx.doi.org/10.14257/ijmue.2017.12.11.01

[52] Nickparvar M. Brain tumor MRI. 2023. Available from: https://www.kaggle.com/datasets/masoudnickparvar/brain-tumor-mri-dataset

[53] Kumar A, Agarwal M, Aquib M. A genetic algorithm-enhanced deep neural network for efficient and optimized brain tumour detection. International Advanced Computing Conference. 311-21.Cham: Springer 2023; pp.
http://dx.doi.org/10.1007/978-981-19-3679-1_24